Research Square

Preprints are preliminary reports that have not undergone peer review.
They should not be considered conclusive, used to inform clinical practice,
or referenced by the media as validated information.

Prioritizing Coastal Conservation Under Rising Seas and Storm Surge: A Coastal Conservation Index for Protected Area Planning

Bahman Moghaddame-Jafari

bmoghadd@gmu.edu

George Mason University

P. J. Ruess

George Mason University

André de Souza de Lima

George Mason University

Celso Ferreira

George Mason University

Research Article

Keywords: Coastal protected areas, Conservation planning, Principal component analysis, Storm surge, Sea level rise, Mid-Atlantic Bight

Posted Date: November 27th, 2026

DOI: https://doi.org/10.21203/rs.3.rs-11167253/v1

License: This work is licensed under a Creative Commons Attribution 4.0 International License.
Read Full License

Additional Declarations: No competing interests reported.

Prioritizing Coastal Conservation Under Rising Seas and Storm Surge: A Coastal Conservation Index for Protected Area Planning

Bahman Moghaddame-Jafari[1]*, P. J. Ruess[1,2], Andre de Souza de Lima[1], Celso Ferreira[1]

[1] Department of Civil, Environmental, and Infrastructure Engineering, College of Engineering and Computing, George Mason University, Fairfax, VA 22030, USA

[2] Department of Atmospheric, Oceanic, and Earth Sciences, College of Science, George Mason University, Fairfax, VA 22030, USA

* Corresponding author: Bahman Moghaddame-Jafari

Email: bmoghadd@gmu.edu

Abstract

Coastal protected areas provide critical ecological services, support biodiversity, and contribute to climate adaptation, yet they are increasingly affected by storm surge, sea level rise (SLR), and human pressures. Our study developed a Coastal Conservation Index (CCI) to prioritize protected areas across the United States Mid-Atlantic Bight (MAB) by integrating physical, ecological, and social indicators. Nineteen indicators were integrated using Principal Component Analysis (PCA) with varimax rotation to reduce dimensionality and identify dominant patterns influencing conservation priority. The analysis incorporated physics-based storm surge and wave simulations of Hurricane Irene under future SLR conditions. Six principal components with eigenvalues greater than one were retained, explaining 67.0% of the total variance. The rotated components represented six dimensions of conservation priority: Human Development, Wave Climate, Conservation Status, Surge Flooding, Flood Depth, and Flood Duration. Rotated component scores were weighted according to their share of retained variance, combined into a composite score,

and normalized to a 0–100 CCI scale. The resulting CCI revealed substantial spatial variation in conservation priority across the MAB, with high-priority protected areas occurring in distinct coastal clusters rather than being uniformly distributed across the region. State-level differences explained substantially more variation in CCI scores than management type, indicating that geographic and environmental conditions were more strongly associated with conservation priority than management designation. The CCI provides a transparent, multidimensional framework for regional screening that can help identify protected areas warranting further evaluation and support more targeted coastal conservation and adaptation planning.

Keywords: Coastal protected areas; Conservation planning; Principal component analysis; Storm surge; Sea level rise; Mid-Atlantic Bight

Length of the manuscript: 7610 words equivalent (including 6 figures and 1 table)

Introduction

Coastal ecosystems provide critical ecological and social benefits, including biodiversity conservation, habitat connectivity, shoreline stabilization, and flood attenuation (Williams et al. 2022; Pascual et al. 2023; Gleason et al. 2023). Many occur within protected areas increasingly affected by urban development, habitat fragmentation, storm surge, and sea level rise (SLR) (Pang et al. 2023; O'Hara et al. 2024; Bernier et al. 2024; Delach et al. 2024). These pressures can alter coastal processes, increase saltwater intrusion, restrict landward ecosystem migration, and degrade wetlands and coastal forests (Smart et al. 2021; Wen and Hughes 2022; Zhong et al. 2024).

Because conservation resources are limited, planning requires approaches that identify locations where management attention may provide the greatest benefits. Conservation prioritization increasingly integrates ecological, environmental, and social information to support spatial decision-making (Armsworth et al. 2020; Watson et al. 2023; Gopalakrishna et al. 2024). Multivariate techniques such as Principal Component Analysis (PCA) can synthesize correlated indicators by reducing dimensionality while retaining dominant patterns of variability (Wu 2021; Saba et al. 2024; Hinojos et al. 2026). However, coastal assessments often consider physical hazards, ecological characteristics, and

anthropogenic pressures separately, limiting their ability to represent the multidimensional conditions relevant to conservation planning.

The United States Mid-Atlantic Bight (MAB) contains extensive coastal protected areas exposed to both coastal hazards and human development. Previous assessments have generally evaluated hydrodynamic hazards, ecological characteristics, and anthropogenic pressures independently (Anderson et al. 2021; Roukounis and Tsihrintzis 2022). Integrating physics-based storm surge and wave simulations under future SLR with ecological and social indicators provides an opportunity to evaluate conservation priority across these interacting dimensions.

Our study develops a Coastal Conservation Index (CCI) that integrates coastal hazard exposure, ecological characteristics, and anthropogenic conditions to identify relative conservation priorities among protected areas across the MAB. We hypothesize that conservation priorities are spatially heterogeneous and reflect the combined influence of these dimensions rather than any single indicator. We address three research questions:

1. Which physical, ecological, and anthropogenic dimensions characterize variation among coastal protected areas in the MAB?
2. Can these characteristics be integrated into a CCI that differentiates relative conservation priorities among protected areas?
3. How are conservation priorities spatially distributed across the MAB, and how do they vary among states and management categories?

By integrating protected area characteristics, human development pressures, and physics-based coastal hazard exposure, the CCI provides a multivariate regional screening framework for comparing protected areas under a consistent SLR planning scenario.

Methodology

Study Area

Our study focuses on the MAB, extending from coastal North Carolina to New York (Fig. 1). The region contains extensive estuarine, barrier-island, wetland, and coastal landscapes and is highly exposed to coastal flooding, wave action, and relative SLR (Lentz et al. 2021;

Hein et al. 2021; Sweet et al. 2022; Lopez et al. 2024). Protected areas were obtained from the Protected Areas Database of the United States (PAD-US) v4.0 (U.S. Geological Survey 2024). We analyzed protected area polygons exposed to Hurricane Irene (2011) storm surge based on the hydrodynamic modeling of Moghaddame-Jafari (2026). Irene provided a consistent regional event because its track and coastal impacts extended across much of the MAB.

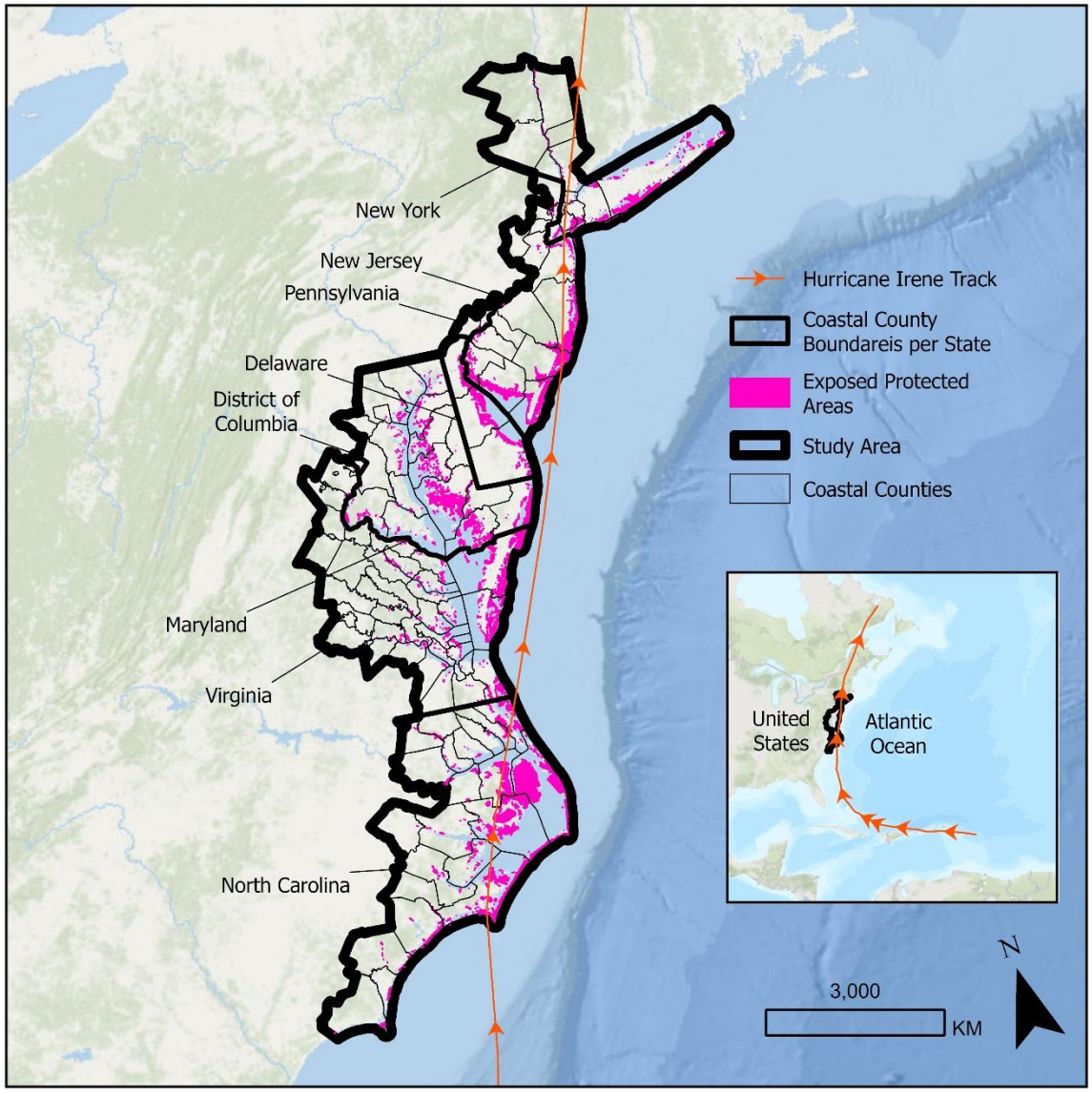


Fig. 1 Spatial distribution of protected areas exposed to Hurricane Irene (2011) storm surge across the MAB

Data Sources and Indicators

Indicators represented three dimensions relevant to coastal conservation prioritization: ecological characteristics, coastal hazard exposure, and anthropogenic conditions. Selection was informed by previous coastal vulnerability, conservation prioritization, and climate adaptation studies (Anderson et al. 2021; Wu 2021; Roukounis and Tsihrintzis 2022; Peck et al. 2022). Following preprocessing and PCA suitability assessment, 19 indicators were retained for CCI development. Ecological indicators characterized protection status, connectivity, and soil drainage; exposure indicators represented storm surge, flooding, waves, sea level trends, tides, nearshore slope, and wind climate; and social indicators represented population, urbanization, transportation, recreation access, and historic resources. Indicator definitions and data sources are summarized in Table 1, with processing methods provided in Supplementary Table S1.

Table 1 Indicators retained for development of the Coastal Conservation Index (CCI), including indicator category, description, data source, and citation

Category	No.	Indicator	Description	Data source / citation
Ecology	1	Level of Protection (GAP Status)	Degree of biodiversity-oriented protection and management intent	PAD-US v4.0 (U.S. Geological Survey 2024)
Ecology	2	Connectivity Potential	Potential landscape connectivity among protected areas	PAD-US v4.0 (U.S. Geological Survey 2024)
Ecology	3	Soil Drainage Capacity	Soil drainage characteristics influencing the potential for prolonged saltwater retention following coastal inundation	NRCS gSSURGO (Soil Survey Staff 2025)
Exposure	4	Nearshore Slope	Coastal slope influencing wave transformation and inundation	Global Nearshore Slope Dataset (Athanasiou et al. 2019)
Exposure	5	Maximum Storm Surge Level	Simulated peak storm surge elevation	ADCIRC outputs (Moghaddame-Jafari 2026)
Exposure	6	Maximum Surge Depth	Maximum simulated surge depth above the ground surface	ADCIRC outputs (Moghaddame-Jafari 2026)

Exposure	7	Maximum Inundation Duration	Maximum duration of inundation during the simulated storm event	ADCIRC outputs (Moghaddame-Jafari 2026)
Exposure	8	Maximum Significant Wave Height	Simulated maximum significant wave height during storm conditions	SWAN outputs (Moghaddame-Jafari 2026)
Exposure	9	Historical Sea Level Trend	Long-term relative sea level trend	NOAA CO-OPS (NOAA CO-OPS 2026)
Exposure	10	Tidal Range	Difference between mean high and low tide levels	NOAA CO-OPS (NOAA CO-OPS 2026)
Exposure	11	ARI Significant Wave Height	Extreme significant wave height associated with recurrence intervals	NACCS (U.S. Army Corps of Engineers 2015)
Exposure	12	ARI Storm Surge Level	Extreme storm surge level associated with recurrence intervals	NACCS (U.S. Army Corps of Engineers 2015)
Exposure	13	Mean Annual Wind Speed	Long-term mean annual wind speed	AORC (NOAA Office of Water Prediction 2023)
Exposure	14	Mean Annual Maximum Hourly Wind Speed	Mean annual maximum hourly wind speed	AORC (NOAA Office of Water Prediction 2023)
Social	15	Population Density (within 1 km)	Human population density surrounding protected areas	LandScan USA (Weber et al. 2022)
Social	16	Distance to Major Roads	Distance from protected areas to major transportation corridors	Transportation (Roads and Railroads) (U.S. Census Bureau 2025)
Social	17	Access to Public Recreation	Public accessibility and recreation opportunity	PAD-US v4.0 (U.S. Geological Survey 2024)
Social	18	Proximity to Historic Sites	Proximity to cultural and historical resources	National Register of Historic Places (National Park Service 2025)
Social	19	Percent Urbanization	Proportion of surrounding developed land cover	Annual NLCD (2024)

Storm Surge Modeling

Storm surge and wave conditions for Hurricane Irene were derived from previously completed ADCIRC+SWAN simulations documented by Moghaddame-Jafari (2026). The model used an OceanMesh2D unstructured mesh and ERA5 atmospheric forcing to simulate water levels and wave conditions across the MAB (Roberts et al. 2019; Hersbach et al. 2020). Model outputs included maximum storm surge level, surge depth, inundation duration, and significant wave height. Inundation was identified using a 0.1-m water-depth threshold to minimize numerical noise associated with shallow flooding. The primary CCI used the 1.3 m NOAA Intermediate SLR scenario for approximately 2100 (Sweet et al. 2022). PCA sensitivity was evaluated using additional Irene simulations at 0.0, 0.6, and 2.1 m SLR. For each scenario, storm surge elevation, inundation duration, and maximum significant wave height were re-extracted, and PCA was repeated using identical preprocessing, standardization, and rotation procedures. We compared eigenvalue spectra, retained components, explained variance, and rotated loadings among scenarios. Because the multivariate structure remained broadly similar, the 1.3 m scenario was retained as the primary planning scenario.

Spatial Processing and Indicator Extraction

GIS processing quantified ecological, exposure, and social characteristics for each protected area. PAD-US and NRCS gSSURGO were used to characterize protection, connectivity, and soil drainage. Hydrodynamic outputs, NOAA tide-gauge observations, NACCS products, and AORC climate data characterized coastal exposure, while LandScan, U.S. Census transportation data, PAD-US recreation attributes, the National Register of Historic Places, and NLCD characterized anthropogenic conditions. Spatial interpolation, raster extraction, zonal statistics, buffers, and proximity analyses were applied as appropriate. Detailed processing for each indicator is provided in Supplementary Table S1.

Principal Component Analysis (PCA)

Principal Component Analysis (PCA) was used to reduce dimensionality and identify dominant covariation among indicators (Jolliffe and Cadima 2016). Prior to PCA, candidate indicators were Yeo–Johnson transformed to reduce skewness and standardized as z-scores. Sampling adequacy was evaluated using the Kaiser–Meyer–Olkin (KMO) measure and Bartlett's test of sphericity, and indicators reducing overall adequacy were removed

during screening. The final dataset contained 19 indicators and 10,918 protected areas. Components with eigenvalues greater than 1.0 were retained using the Kaiser criterion, followed by orthogonal varimax rotation to improve interpretability (Kaiser 1958). Rotated components were interpreted from the magnitude, direction, and conceptual meaning of their dominant indicator loadings. Because PCA component signs are mathematically arbitrary, each retained rotated component was evaluated before CCI aggregation. Components were oriented so that positive scores represented increasing magnitude of the conservation-relevant dimension represented by that component. The native orientations of all six components were consistent with their intended interpretations; therefore, no sign reversals were required.

Coastal Conservation Index (CCI) Development

The CCI was developed as a regional screening tool integrating coastal hazard exposure, ecological characteristics, and anthropogenic conditions. Higher scores represent stronger combined expression of these conservation-relevant dimensions and identify protected areas that may warrant further assessment or planning rather than prescribing management actions or investment levels.

Each protected area received a score for each retained rotated component. Component j was weighted according to the variance represented by its rotated loading structure:

$$V_j = \sum_{p=1}^{P} l_{pj}^2$$

and normalized across the K retained components:

$$w_j = \frac{V_j}{\sum_{k=1}^{K} V_k}$$

where l_{ij} is the rotated loading of indicator i on component j. Weights sum to one and represent each component's share of variance within the retained rotated solution; they do not imply greater conservation importance.

The raw CCI for protected area i was calculated as:

$$CCI_{raw,i} = \sum_{j=1}^{K} (w_j \times RC_{ij})$$

where RC_{ij} is the oriented rotated-component score. Raw scores were min–max normalized to 0–100:

$$CCI_i = 100 \times \frac{CCI_{raw,i} - CCI_{raw,min}}{CCI_{raw,max} - CCI_{raw,min}}$$

The resulting CCI represents relative priority within the analyzed MAB protected area network. Protected areas at or above the regional 90th percentile were identified as the top 10% of the CCI distribution for regional comparison; this cutoff represents a relative ranking rather than an ecological or management threshold. For interpretation, the dominant CCI dimension of each protected area was identified as the rotated component with the largest weighted contribution to its raw CCI. Weighting sensitivity was evaluated by recalculating the CCI with equal component weights and comparing rankings using Spearman correlation and overlap between the respective top-10% sets.

Statistical Analysis and Group Comparisons

CCI distributions were compared among states and management categories using descriptive statistics and Welch ANOVA, which accommodates unequal group sizes and variances (Welch 1951). Effect sizes were reported to characterize the magnitude of group differences. Because neighboring protected areas may share environmental and anthropogenic conditions, inferential results were interpreted primarily as regional group comparisons rather than spatially independent estimates.

Protected areas were treated as individual observational units regardless of spatial extent because the CCI was developed for protected area-level prioritization. Significant Welch ANOVA results were followed by Games–Howell pairwise comparisons (Games and Howell 1976). Groups with fewer than 100 observations were excluded from inferential tests but retained for descriptive and spatial analyses. Group sample sizes, inclusion criteria, Welch ANOVA results, and Games–Howell comparisons are provided in Supplementary Tables S4–S6.

Results

PCA Suitability

The final PCA dataset included 10,918 protected areas and 19 ecological, exposure, and social indicators. The overall Kaiser–Meyer–Olkin (KMO) measure of sampling adequacy was 0.748, indicating adequate shared variance among the indicators for PCA. Bartlett's test of sphericity was highly significant, $\chi^2(171) = 105{,}084.02$, $p < 0.001$, rejecting the null hypothesis that the correlation matrix was an identity matrix and confirming that sufficient intercorrelation existed among the indicators for component extraction. These diagnostics supported application of PCA to identify the dominant multivariate patterns among the indicators.

PCA Sensitivity to SLR

The sensitivity of the PCA structure to SLR was evaluated using Hurricane Irene simulations under 0.0, 0.6, 1.3, and 2.1 m SLR scenarios. As sea level increased, both the number and area of protected areas exposed to storm surge increased across the MAB (Moghaddame-Jafari 2026). Despite the increase in exposure, the eigenvalue distributions remained broadly similar across the four scenarios (Fig. 2). The 0.0 and 0.6 m scenarios retained five components under the Kaiser criterion ($\lambda > 1$), whereas the 1.3 and 2.1 m scenarios retained six. The emergence of a sixth component under higher SLR indicates some sensitivity of the PCA structure to increasing flood exposure, while the similarity of the overall eigenvalue patterns suggests that the dominant dimensions of variability remained generally stable. The 1.3 m NOAA Intermediate scenario was retained for development of the final CCI as the primary planning scenario evaluated in our study.

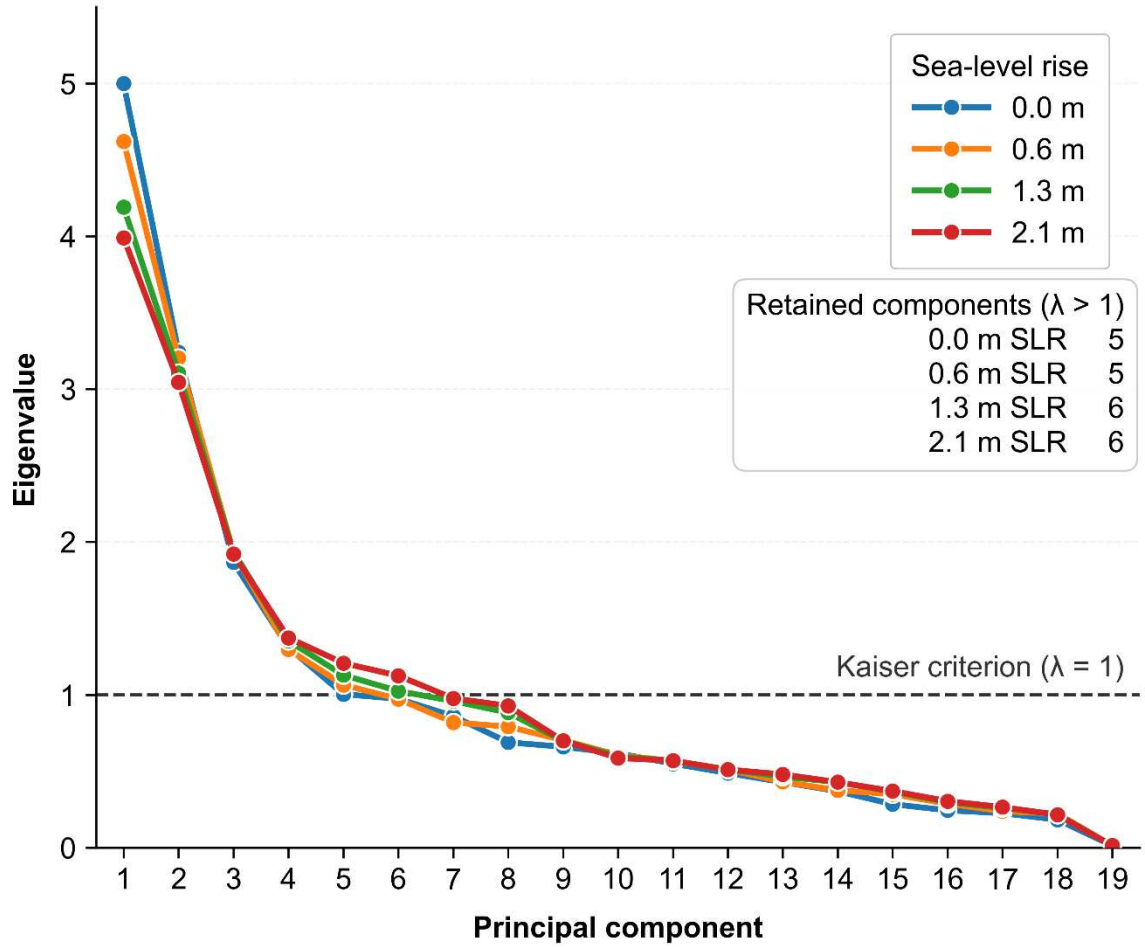


Fig. 2 Principal component eigenvalues across Hurricane Irene simulations under 0.0, 0.6, 1.3, and 2.1 m SLR scenarios in the MAB. The dashed horizontal line represents the Kaiser criterion (λ = 1). Five components were retained under the 0.0 and 0.6 m scenarios and six under the 1.3 and 2.1 m scenarios

Component Extraction and Variance Explained

Six principal components (PCs) with eigenvalues greater than 1.0 were retained according to the Kaiser criterion for the 1.3 m SLR scenario (Fig. 3). Together, the six retained components explained approximately 67.0% of the total variance among the 19 standardized indicators. The first two components accounted for the largest proportions of variance, followed by progressively smaller contributions from the remaining retained components. Components beyond PC6 had eigenvalues below 1.0 and were therefore not retained.

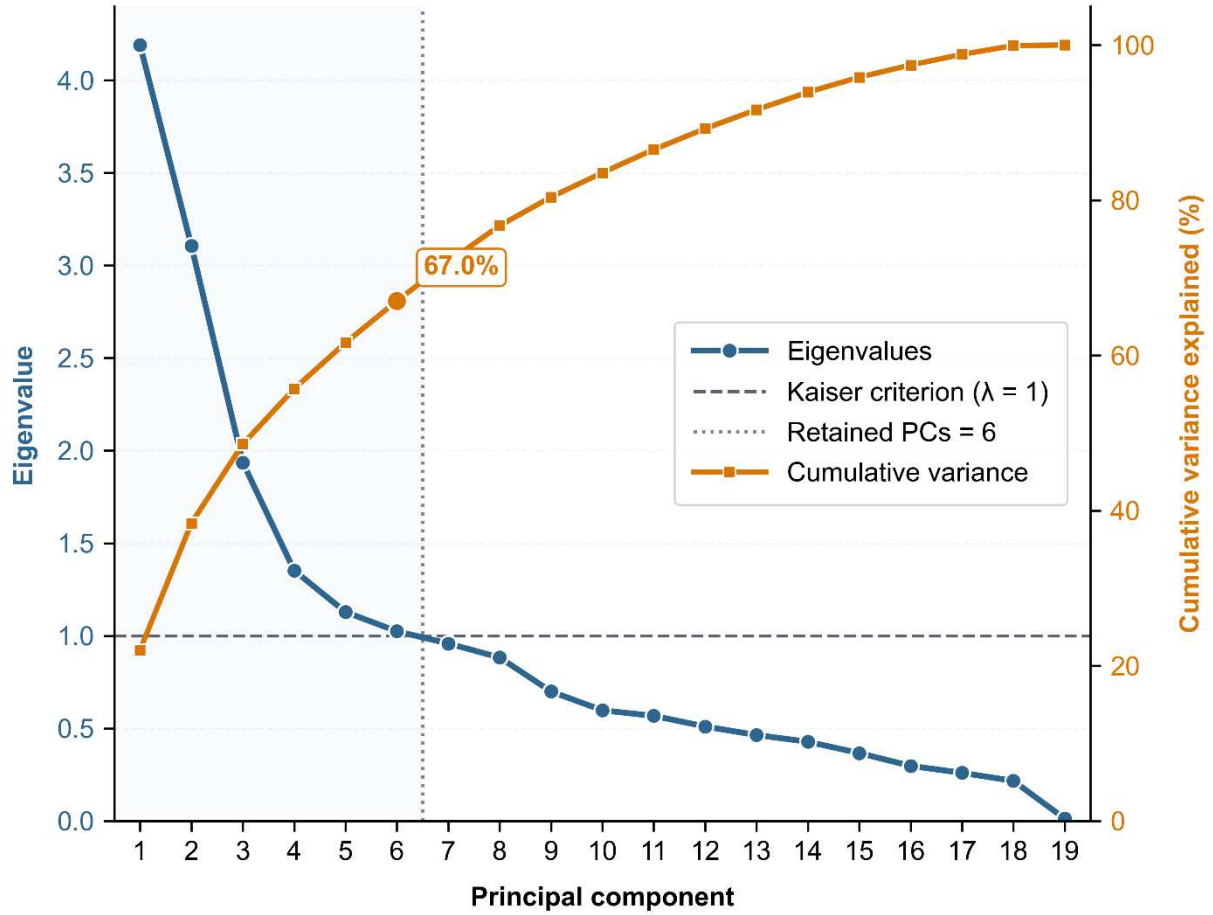


Fig. 3 Scree plot of PCA results for the 1.3 m SLR scenario showing eigenvalues and cumulative explained variance across the 19 indicators used in CCI development. The horizontal dashed line represents the Kaiser criterion (λ = 1), and the vertical dotted line identifies the six retained principal components. The six retained components collectively explained approximately 67.0% of the total variance

Orthogonal varimax rotation was subsequently applied to the six-component solution to improve interpretability while preserving the total variance represented by the retained solution. The resulting rotated structure produced six interpretable dimensions characterized by distinct combinations of ecological, exposure, and social indicators. Detailed eigenvalues, explained variance, rotated-component variance, and corresponding CCI weights are provided in Supplementary Table S2.

Rotated Component Interpretation

Following varimax rotation, the six retained components represented distinct dimensions of coastal conservation conditions across the MAB. Component interpretation was based

on the magnitude, direction, and conceptual meaning of the dominant indicator loadings. The complete rotated component loading matrix and component themes are provided in Supplementary Table S3.

RC1 represented Human Development and was characterized by strong positive loadings for population density (0.832) and access to public recreation (0.689), together with negative loadings for distance to major roads (−0.784) and proximity to historic sites (−0.634). Historical sea-level trend also exhibited a negative loading (−0.520). Higher RC1 scores therefore characterized protected areas associated with greater surrounding population and accessibility.

RC2 represented Wave Climate and was dominated by mean annual wind speed (0.932), mean annual maximum hourly wind speed (0.930), ARI significant wave height (0.692), and maximum significant wave height (0.569). Maximum storm surge level also contributed positively (0.519). Higher RC2 scores therefore characterized protected areas associated with stronger wind conditions and more energetic wave environments.

RC3 represented Conservation Status and was characterized by a strong positive loading for level of protection based on GAP status (0.780), together with negative loadings for Soil Drainage Capacity (−0.760) and percent urbanization (−0.654). Connectivity potential also exhibited a moderate positive loading (0.456). Higher RC3 scores therefore generally characterized protected areas with stronger biodiversity-oriented protection, lower surrounding urbanization, greater connectivity, and poorer soil drainage.

RC4 represented Surge Flooding and was characterized by strong positive loadings for ARI storm surge level (0.829) and tidal range (0.816), with an additional positive contribution from maximum storm surge level (0.493). Higher RC4 scores therefore characterized protected areas associated with greater extreme surge levels and tidal influence.

RC5 represented Flood Depth and was dominated by maximum surge depth (0.848), with maximum significant wave height also exhibiting a strong positive loading (0.586). Higher RC5 scores therefore characterized protected areas experiencing greater modeled surge depths and wave exposure.

RC6 represented Flood Duration and was dominated by maximum inundation duration (0.748). Nearshore slope exhibited a moderate negative loading (−0.438), while maximum storm surge level exhibited a moderate positive loading (0.399). Higher RC6 scores therefore primarily characterized protected areas experiencing longer-lasting inundation, with secondary associations with coastal slope and storm surge conditions.

Some indicators contributed to more than one rotated component, reflecting interactions among coastal processes. Maximum significant wave height, for example, loaded similarly on RC2 (0.569) and RC5 (0.586), while maximum storm surge level contributed to RC2 (0.519), RC4 (0.493), and RC6 (0.399). These cross-loadings were retained because they reflect the interconnected nature of wave, surge, and inundation processes rather than independent environmental conditions.

Coastal Conservation Index (CCI)

The CCI integrated the six weighted rotated components into a single multidimensional conservation prioritization metric normalized to a 0–100 scale. CCI scores varied substantially across the 10,918 protected areas (Fig. 4). The distribution spanned the full normalized range, indicating considerable variation in relative conservation priority across the MAB. The 90th percentile was used to identify protected areas within the top 10% of CCI scores.

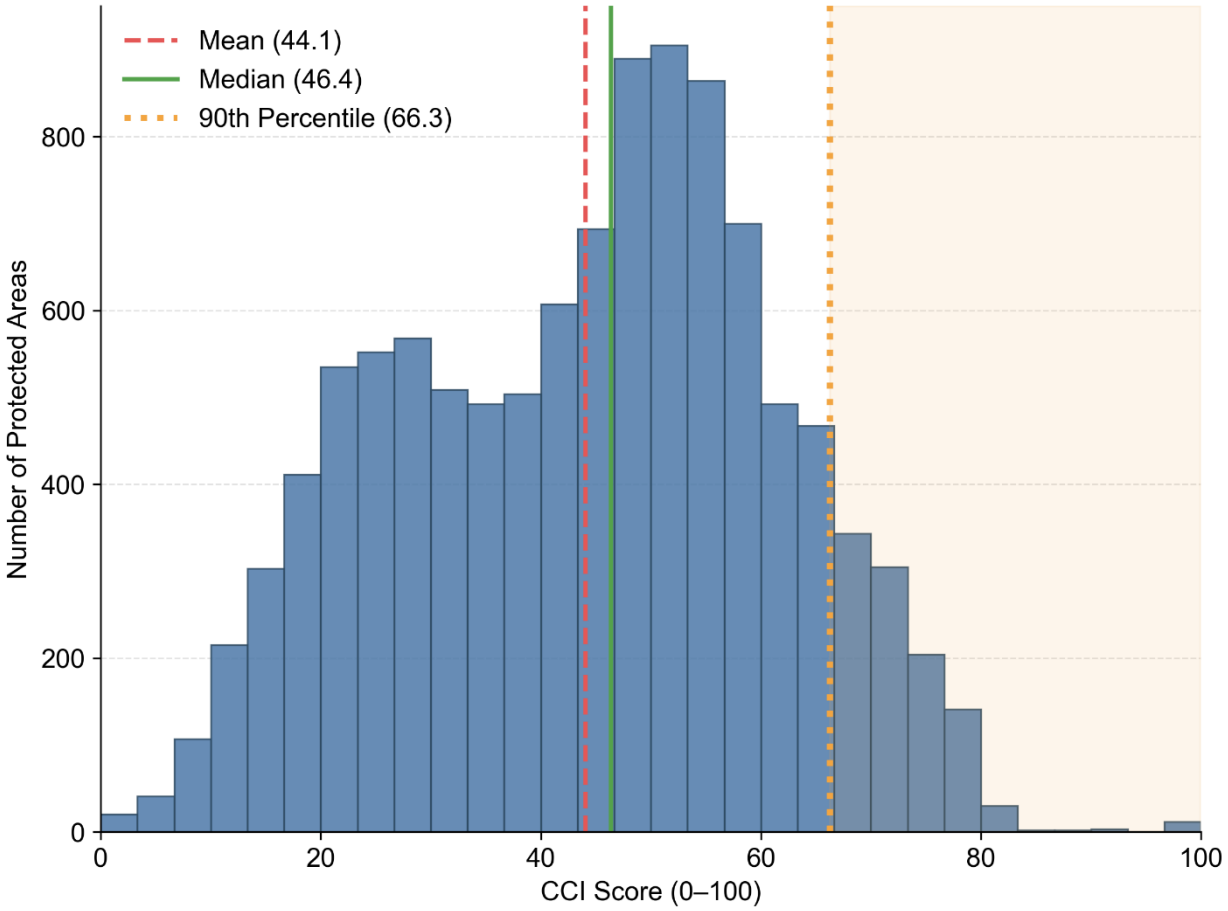


Fig. 4 Distribution of normalized Coastal Conservation Index (CCI) scores across 10,918 protected areas in the Mid-Atlantic Bight. Vertical lines indicate the mean, median, and 90th-percentile threshold defining the top 10% of CCI scores. Higher CCI scores indicate greater relative conservation priority

Spatial patterns in CCI scores were heterogeneous across the MAB (Fig. 5). Higher-priority protected areas occurred in distinct coastal clusters rather than being uniformly distributed throughout the region. Concentrations of relatively high CCI scores were evident along portions of New York and New Jersey and within several coastal areas of Virginia and North Carolina. In contrast, many protected areas surrounding the Chesapeake Bay and portions of Maryland exhibited lower CCI scores. State-specific maps are provided in Supplementary Figures S1–S8. Additionally, CCI rankings were highly consistent under equal component weighting (Spearman's $\rho = 0.971$, $p < 0.001$), with 82.4% overlap among protected areas classified in the top 10% under the variance-weighted and equal-weight approaches.

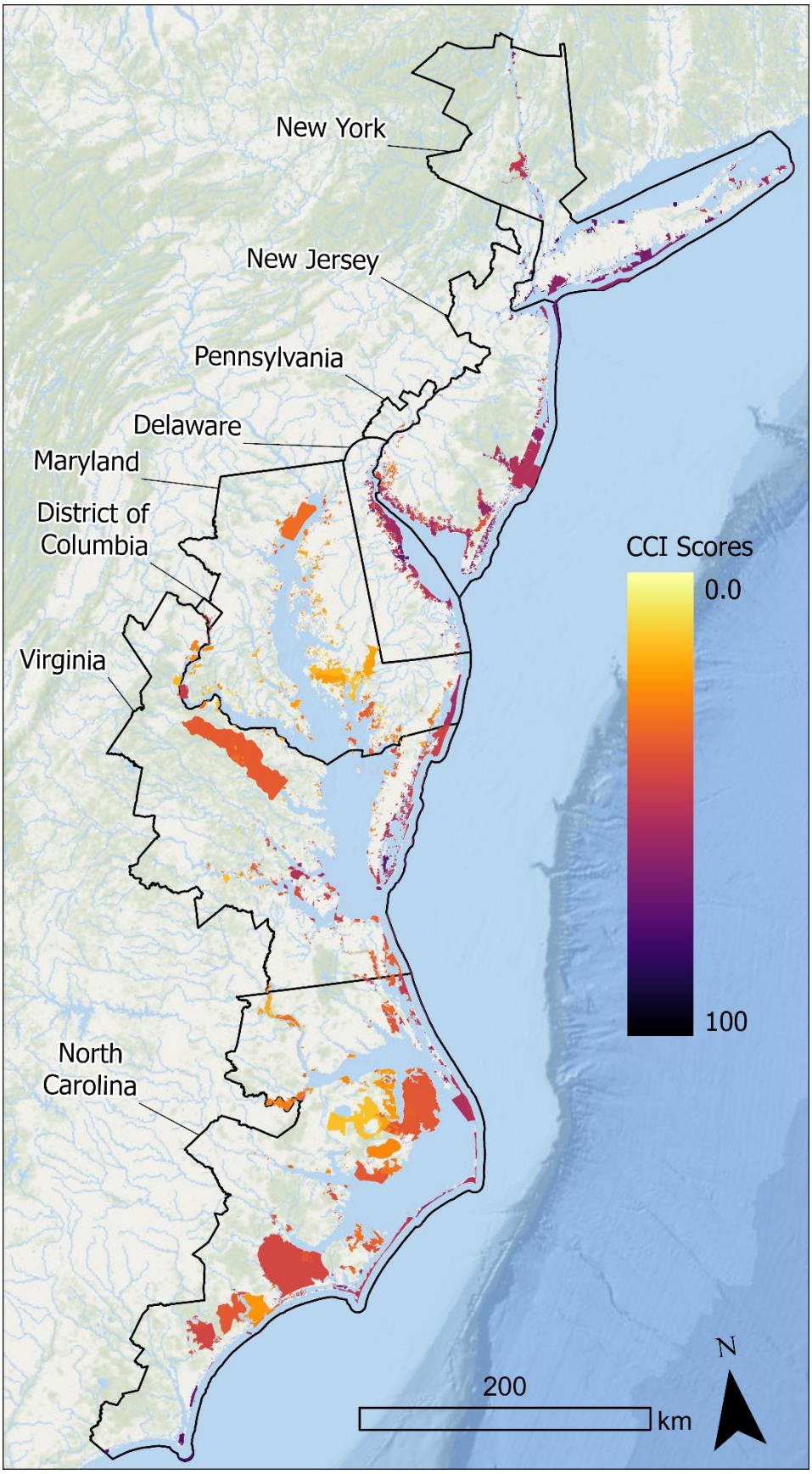

New York
New Jersey
Pennsylvania
Delaware
Maryland
District of Columbia
Virginia
North Carolina
CCI Scores
0.0
100
200
km
N

Fig. 5 Spatial distribution of Coastal Conservation Index (CCI) scores across protected areas in the Mid-Atlantic Bight. CCI scores range from 0 to 100, with higher values indicating greater relative conservation priority

The dominant contribution to the CCI varied among protected areas, indicating that composite scores reflected different underlying dimensions across the MAB. Human Development and Wave Climate were the most frequently dominant dimensions, accounting for 27.7% and 27.2% of protected areas, respectively, followed by Conservation Status (18.7%), Surge Flooding (11.9%), Flood Duration (11.0%), and Flood Depth (3.6%).

The distribution of protected areas within the top 10% of CCI scores differed when evaluated by number and total area (Fig. 6). Management and state groups containing numerous top 10% protected areas did not necessarily contain the greatest total area, reflecting differences in protected area size among groups.

Geographic differences showed a similar pattern. New York contained the greatest total high-priority area (254 km^2; n = 625), followed by New Jersey (168 km^2; n = 335) and North Carolina (150 km^2; n = 54). Although North Carolina contained considerably fewer high-priority protected areas than New York or New Jersey, its high-priority sites represented a substantial total area. Delaware contained 70 km^2 across 75 high-priority protected areas, while Virginia contained 30 km^2 across three protected areas. No protected areas exceeded the 90th-percentile threshold in Maryland, Pennsylvania, or the District of Columbia.

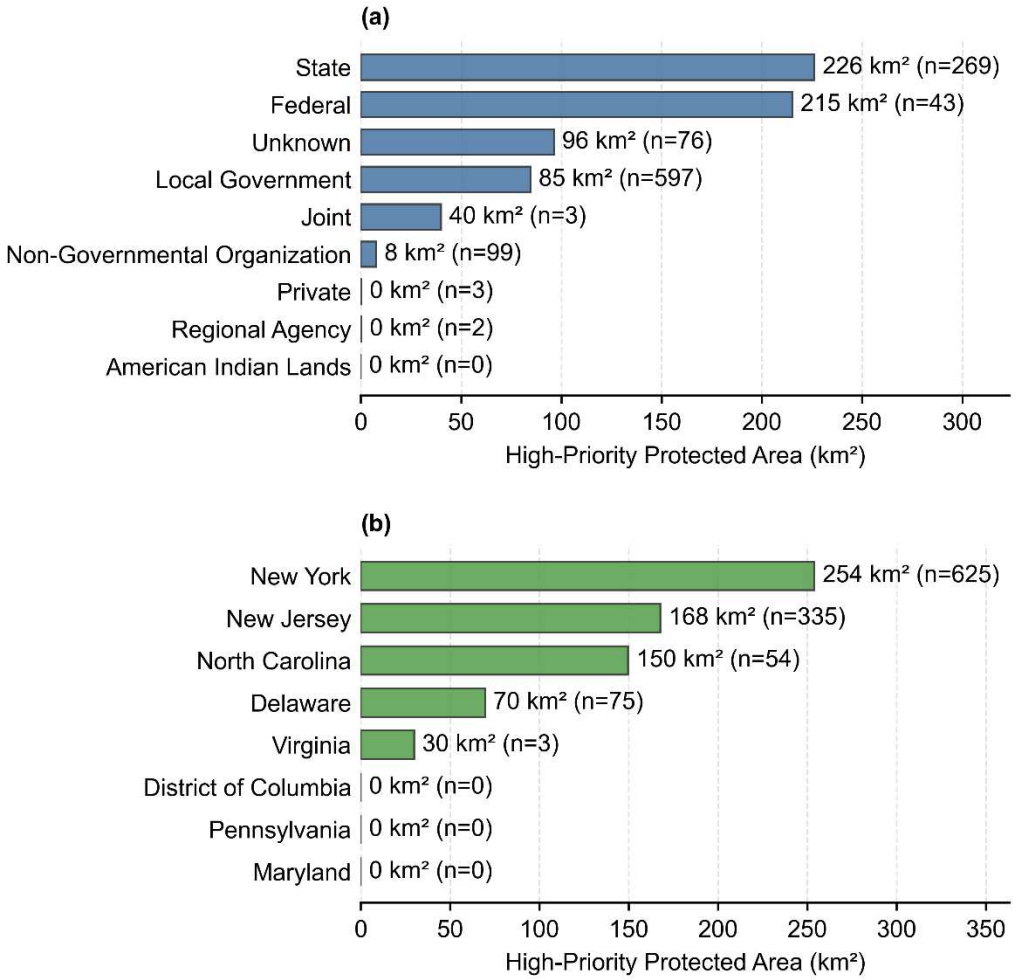


Fig. 6 Distribution of protected areas within the top 10% of CCI scores by (a) management type and (b) state across the MAB. Bar lengths represent their total area (km^2), and labels report the corresponding number of protected areas (n)

Significance Tests

Welch ANOVA indicated significant differences in CCI scores among both management types and states in the MAB. CCI scores differed significantly among management types, $F(5, 2032.27) = 353.07$, $p < 0.001$, with a partial η^2 of 0.117. State-level differences were substantially greater, $F(5, 3974.54) = 4273.39$, $p < 0.001$, with a partial η^2 of 0.592. These results indicate that geographic differences among states accounted for substantially more variation in CCI scores than management type (Supplementary Table S4).

Games–Howell comparisons further demonstrated substantial differences among management types (Supplementary Table S5). The largest standardized difference occurred between Joint and Local Government protected areas ($|g| = 1.73$), followed by

Joint and Unknown (|g| = 1.26), Joint and Non-Governmental Organization (|g| = 1.26), and Federal and Joint (|g| = 1.22). In contrast, Federal and Unknown protected areas showed little difference (g = 0.04, p = 0.954), as did Federal and Non-Governmental Organization protected areas (g = 0.09, p = 0.403).

State-level contrasts were even more pronounced (Supplementary Table S6). The largest standardized difference occurred between Maryland and New York (|g| = 4.29), followed by Delaware and Maryland (|g| = 3.40) and Maryland and New Jersey (|g| = 2.73). In contrast, Delaware and New Jersey exhibited nearly identical CCI distributions (g = 0.02, p = 0.996), as did North Carolina and Virginia (g = 0.03, p = 0.972). Overall, the substantially larger state effect supports strong geographic structuring of conservation priority across the MAB.

Discussion

Synthesis of Hazard, Ecological, and Human Interaction

The PCA indicates that conservation priority across MAB protected areas reflects distinct but complementary physical, ecological, and anthropogenic dimensions. Notably, coastal hazards separated into Wave Climate, Surge Flooding, Flood Depth, and Flood Duration, indicating that coastal exposure cannot be represented fully by a single hazard metric. Protected areas experiencing high surge levels, for example, may not experience the greatest flood depths or longest inundation durations because these responses reflect interacting hydrodynamic and geomorphic processes (Pang et al. 2023; Bernier et al. 2024).

The separation of these hazard dimensions from Human Development and Conservation Status further demonstrates the value of integrating physical exposure with surrounding ecological and anthropogenic conditions. Similar multidimensional approaches have shown that population, infrastructure, ecological condition, and physical exposure provide complementary information for coastal vulnerability and conservation planning (Anderson et al. 2021; Wu 2021; Xiang et al. 2024). Consequently, protected areas with similar CCI scores may reflect different combinations of underlying conditions, reinforcing interpretation of the CCI as a multidimensional regional prioritization framework rather than a measure of any single hazard or conservation characteristic.

Regional Variability in Conservation Priority

Conservation priorities exhibited strong geographic variation across the MAB. State-level differences in CCI scores were substantially greater than differences among management types, as indicated by the larger effect size for state (partial $\eta^2 = 0.592$) than management type (partial $\eta^2 = 0.117$). Protected areas within the top 10% of the regional CCI distribution were also spatially clustered rather than uniformly distributed across the MAB, reflecting geographic variation in the physical, ecological, and anthropogenic conditions represented by the CCI.

The number and total area of protected areas within the top 10% of CCI scores revealed different geographic patterns, highlighting the influence of protected area size and fragmentation on regional comparisons. States with relatively few large protected areas may contain substantial top 10% CCI area, whereas states with numerous smaller protected areas may show the opposite pattern. State boundaries do not themselves determine CCI scores; rather, state-level comparisons summarize geographic variation in the conditions represented by the index. Individual protected area scores therefore remain the appropriate unit for identifying locations that warrant further evaluation.

Management and Planning Implications

The distribution of protected areas within the top 10% of CCI scores differed among management types when evaluated by number and total area. Management categories containing relatively few large protected areas may account for substantial top 10% CCI area, whereas categories containing numerous smaller sites may show the opposite pattern. These differences suggest that planning needs may vary between management contexts characterized by large individual protected areas and those involving numerous smaller, dispersed sites.

The multidimensional structure of the CCI also supports a two-stage approach to planning. The overall CCI can first identify protected areas with relatively high regional priority, while the underlying component scores can indicate which dimensions contribute most strongly to individual scores. For example, protected areas influenced primarily by flood depth and duration may require different considerations than those characterized by human development pressure or conservation status. This approach preserves a consistent

regional screening metric while retaining information needed to interpret the conditions underlying individual CCI scores.

Conclusions

Our study developed a multidimensional CCI integrating physical hazard, ecological, and anthropogenic indicators to prioritize coastal protected areas across the MAB. PCA identified six distinct dimensions, and the resulting CCI revealed substantial geographic variation in conservation priority. Protected areas within the top 10% of CCI scores were spatially clustered, and differences among states were substantially greater than those among management types, emphasizing the geographic structure of the conditions represented by the index.

The CCI is intended as a regional screening tool and does not capture all factors relevant to site-specific decisions, including management feasibility, costs, land-use constraints, species-specific responses, and local adaptation capacity. Coastal exposure indicators also reflect Hurricane Irene and therefore do not represent the full range of possible storm conditions. Accordingly, the CCI can identify protected areas warranting further evaluation, while the underlying component scores provide insight into the conditions contributing to their relative priority. The framework can be updated with new data and adapted to other coastal regions to support multidimensional conservation planning under SLR.

Acknowledgments

The authors acknowledge the Texas Advanced Computing Center (TACC) at The University of Texas at Austin for providing HPC resources on Stampede3. This work was supported by National Science Foundation ACCESS allocation CIV260026.

References

Anderson CC, Renaud FG, Hagenlocher M, Day JW (2021) Assessing Multi-Hazard Vulnerability and Dynamic Coastal Flood Risk in the Mississippi Delta: The Global

Delta Risk Index as a Social-Ecological Systems Approach. Water 13:577. https://doi.org/10.3390/w13040577

Armsworth PR, Benefield AE, Dilkina B, et al (2020) Allocating resources for land protection using continuous optimization: biodiversity conservation in the United States. Ecological Applications 30:e02118. https://doi.org/10.1002/eap.2118

Athanasiou P, van Dongeren A, Giardino A, et al (2019) Global distribution of nearshore slopes with implications for coastal retreat. Earth System Science Data 11:1515–1529. https://doi.org/10.5194/essd-11-1515-2019

Bernier NB, Hemer M, Mori N, et al (2024) Storm surges and extreme sea levels: Review, establishment of model intercomparison and coordination of surge climate projection efforts (SurgeMIP). Weather and Climate Extremes 45:100689. https://doi.org/10.1016/j.wace.2024.100689

Delach A, Nunes LA, Borowicz A, Weber TC (2024) Designated critical habitats for U.S. imperiled species are not protected from climate and land-use change. Geography and Sustainability 5:482–490. https://doi.org/10.1016/j.geosus.2024.06.001

Games PA, Howell JF (1976) Pairwise Multiple Comparison Procedures with Unequal N's and/or Variances: A Monte Carlo Study. Journal of Educational Statistics 1:113–125. https://doi.org/10.3102/10769986001002113

Gleason MG, Reynolds MD, Heady WN, et al (2023) The importance of identifying and protecting coastal wildness. Front Conserv Sci 4:. https://doi.org/10.3389/fcosc.2023.1224618

Gopalakrishna T, Visconti P, Lomax G, et al (2024) Optimizing restoration: A holistic spatial approach to deliver Nature's Contributions to People with minimal tradeoffs and maximal equity. Proceedings of the National Academy of Sciences 121:e2402970121. https://doi.org/10.1073/pnas.2402970121

Hein CJ, Fenster MS, Gedan KB, et al (2021) Leveraging the Interdependencies Between Barrier Islands and Backbarrier Saltmarshes to Enhance Resilience to Sea-Level Rise. Front Mar Sci 8:. https://doi.org/10.3389/fmars.2021.721904

Hersbach H, Bell B, Berrisford P, et al (2020) The ERA5 global reanalysis. Quarterly Journal of the Royal Meteorological Society 146:1999–2049. https://doi.org/10.1002/qj.3803

Hinojos S, Roscoe K, Grady C (2026) Examining the role of indicators and scale in social vulnerability index construction: A comparative geospatial analysis of inductive and hierarchical models. Applied Geography 186:103822. https://doi.org/10.1016/j.apgeog.2025.103822

Jolliffe IT, Cadima J (2016) Principal component analysis: a review and recent developments. Philos Trans A Math Phys Eng Sci 374:20150202. https://doi.org/10.1098/rsta.2015.0202

Kaiser HF (1958) The Varimax Criterion for Analytic Rotation in Factor Analysis. Psychometrika 23:187–200. https://doi.org/10.1007/BF02289233

Lentz EE, Zeigler SL, Thieler ER, Plant NG (2021) Probabilistic patterns of inundation and biogeomorphic changes due to sea-level rise along the northeastern U.S. Atlantic coast. Landscape Ecol 36:223–241. https://doi.org/10.1007/s10980-020-01136-z

Lopez H, Lee S-K, West R, et al (2024) Projected increase in the frequency of extremely active Atlantic hurricane seasons. Science Advances 10:eadq7856. https://doi.org/10.1126/sciadv.adq7856

Moghaddame-Jafari B (2026) Protected Area Storm Surge Exposure under Sea Level Rise Scenarios in the U.S. Mid-Atlantic Bight

National Park Service (2025) National Register of Historic Places

NOAA CO-OPS (2026) U.S. Relative Sea Level Trends

NOAA Office of Water Prediction (2023) Analysis of Record for Calibration (AORC), Version 1.1

O'Hara CC, Frazier M, Valle M, et al (2024) Cumulative human impacts on global marine fauna highlight risk to biological and functional diversity. PLoS One 19:e0309788. https://doi.org/10.1371/journal.pone.0309788

Pang T, Wang X, Nawaz RA, et al (2023) Coastal erosion and climate change: A review on coastal-change process and modeling. Ambio 52:2034–2052. https://doi.org/10.1007/s13280-023-01901-9

Pascual U, Balvanera P, Anderson CB, et al (2023) Diverse values of nature for sustainability. Nature 620:813–823. https://doi.org/10.1038/s41586-023-06406-9

Peck AJ, Adams SL, Armstrong A, et al (2022) A new framework for flood adaptation: introducing the Flood Adaptation Hierarchy - Ecology & Society. Ecology and Society 27:. https://doi.org/10.5751/ES-13544-270405

Roberts KJ, Pringle WJ, Westerink JJ (2019) OceanMesh2D 1.0: MATLAB-based software for two-dimensional unstructured mesh generation in coastal ocean modeling, Geosci. Model Dev. (GMD), https://doi.org/10.519 /gmd-12-1847-2019.

Roukounis CN, Tsihrintzis VA (2022) Indices of Coastal Vulnerability to Climate Change: a Review. Environ Process 9:29. https://doi.org/10.1007/s40710-022-00577-9

Saba JA, Ash K, Napton D (2024) Assessing the vulnerability of Cape Coral, Florida, to sea level rise using principal component analysis (2020–2050). International Journal of Disaster Risk Reduction 115:105014. https://doi.org/10.1016/j.ijdrr.2024.105014

Smart LS, Vukomanovic J, Sills EO, Sanchez G (2021) Cultural ecosystem services caught in a 'coastal squeeze' between sea level rise and urban expansion. Global Environmental Change 66:102209. https://doi.org/10.1016/j.gloenvcha.2020.102209

Soil Survey Staff (2025) Gridded Soil Survey Geographic (gSSURGO) Database for the United States of America and the Territories, Commonwealths, and Island Nations served by the USDA Natural Resources Conservation Service

Sweet WV, B.D. Hamlington REK, C.P. Weaver PLB, D. Bekaert WB (2022) 2022: Global and Regional Sea Level Rise Scenarios for the United States: Updated Mean Projections and Extreme Water Level Probabilities Along U.S. Coastlines. NOAA Technical Report NOS 01

U.S. Army Corps of Engineers (2015) North Atlantic Coast Comprehensive Study: Resilient Adaptation to Increasing Risk. U.S. Army Corps of Engineers, New York District, New York, NY

U.S. Census Bureau (2025) Transportation (Roads and Railroads)

U.S. Geological Survey (2024) Protected Areas Database of the United States (PAD-US) 4

Watson JEM, Venegas-Li R, Grantham H, et al (2023) Priorities for protected area expansion so nations can meet their Kunming-Montreal Global Biodiversity Framework commitments. Integrative Conservation 2:140–155. https://doi.org/10.1002/inc3.24

Weber E, Moehl J, Weston S, et al (2022) LandScan USA 2021

Welch BL (1951) ON THE COMPARISON OF SEVERAL MEAN VALUES: AN ALTERNATIVE APPROACH. Biometrika 38:330–336. https://doi.org/10.1093/biomet/38.3-4.330

Wen L, Hughes MG (2022) Coastal Wetland Responses to Sea Level Rise: The Losers and Winners Based on Hydro-Geomorphological Settings. Remote Sensing 14:1888. https://doi.org/10.3390/rs14081888

Williams BA, Watson JEM, Beyer HL, et al (2022) Global rarity of intact coastal regions. Conserv Biol 36:e13874. https://doi.org/10.1111/cobi.13874

Wu T (2021) Quantifying coastal flood vulnerability for climate adaptation policy using principal component analysis. Ecological Indicators 129:108006. https://doi.org/10.1016/j.ecolind.2021.108006

Xiang Z, Li Y, Zhang Z (2024) Global conservation priorities of coastal habitats towards extreme sea level rise risks. Journal of Cleaner Production 473:143455. https://doi.org/10.1016/j.jclepro.2024.143455

Zhong J, Liang C, Zhao Y, et al (2024) Identifying loss threshold and migration trajectory in the management of *Suaeda salsa* wetland under coastal squeeze. Marine Environmental Research 194:106329. https://doi.org/10.1016/j.marenvres.2023.106329

(2024) Annual National Land Cover Database | U.S. Geological Survey. https://www.usgs.gov/centers/eros/science/annual-national-land-cover-database. Accessed 7 Feb 2025